SPACE WEATHERING AT LUNAR SWIRLS AND AT HIGH LUNAR LATITUDES Doug Hemingway[1] (djheming@ucsc.edu) and Ian Garrick-Bethell[1,2], [1]Earth & Planetary Sciences, University of California Santa Cruz, 1156 High Street, Santa Cruz, California, 95064, [2]School of Space Research, Kyung Hee University, South Korea.

Summary: Space weathering processes, which gradually alter the optical properties of surfaces exposed directly to the space environment, have important consequences for the interpretation of remote sensing data and thus the characterization of bodies throughout the solar system [1,2]. Direct exposure to solar wind and micrometeoroid bombardment are thought to be the dominant sources of space weathering, however, their relative effects and efficiencies are not yet well understood [1–4].

We investigate how space weathering effects differ at high lunar latitudes, where both solar wind and micrometeoroid flux are reduced (see below), and at lunar swirls (e.g., Fig. 1a), where micrometeoroid flux is unaffected, but where solar wind flux is likely reduced [5,6]. In both cases, we observe similar spectral trends that may have important implications for how space weathering operates.

Background: Both micrometeoroid impacts and solar wind sputtering cause the accumulation of nanophase iron particles on the surfaces of regolith grains [2], leading to albedo reduction, suppression of spectral features, and a more red-sloped continuum (collectively, these effects can be termed optical maturity). However, some meteoroid impacts also decrease optical maturity by exposing fresh material, which then gradually matures until it reaches the steady state, background optical characteristics (herein 'saturation color', for simplicity). The saturation color is not the same everywhere on the Moon and is strongly influenced by the local mineralogy. If the flux of weathering agents is important, then saturation color may also depend on latitude since maximum flux occurs at the equator (both solar wind and micrometeoroids come primarily from within the ecliptic).

Analysis:

Background weathering: Space weathering trends can be characterized by plots of 750 nm reflectance versus the ratio of 950 nm-to-750 nm reflectance [7,8] (Fig. 1b), the former representing albedo and the latter serving as a proxy for both the near-infrared continuum slope and the 1 μm iron absorption feature [9]. Pixels from a region with nearly uniform composition (e.g., the red rectangle in Fig. 1a) will correspond to a steeply sloping cluster of points in the 750 nm vs. 950 nm/750 nm plot (the red dots in Fig. 1b). Points in the lower right of the red point cloud in Fig. 1b correspond to material recently exposed by impacts, and points in the upper left end of the range represent the background color that is reached with maximum (saturation) optical maturity. Since the majority of pixels in any given region will be near saturation maturity, the median point in each cluster (black circles in Fig. 1b) is a reasonable estimate for the saturation color in a given region.

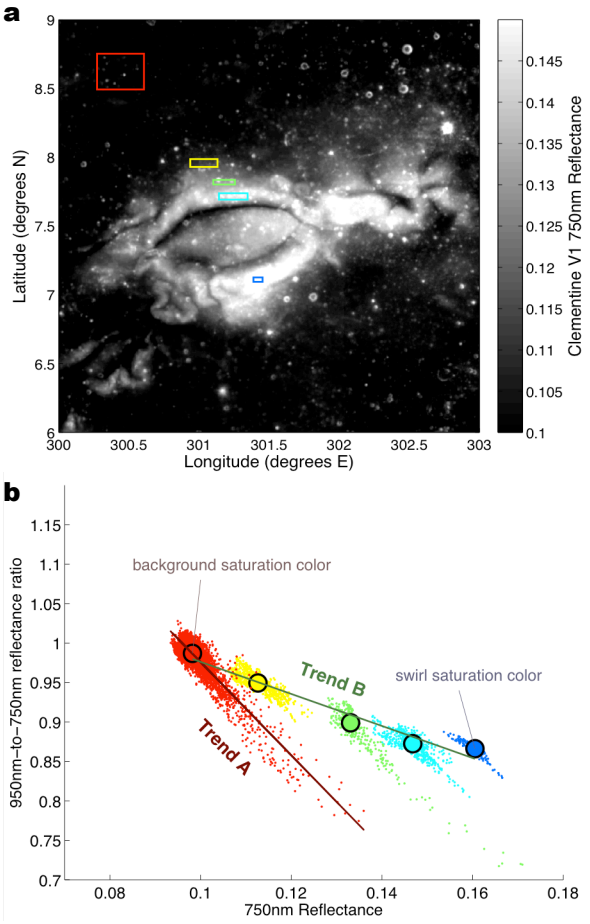

Figure 1: **(a)** Reiner Gamma swirl. **(b)** Spectral characteristics of the pixels sampled from the five rectangular regions (with corresponding colors) shown in (a). The red point cloud corresponds to a representative background region whereas the dark blue point cloud corresponds to the brightest part of the swirl. The dark green line (Trend B) is a best fit through the centroids (black circles) of each cluster. The black circles represent the steady-state, saturation colors reached with maximum optical maturity in each region.

Weathering at swirls: In addition to the red point cluster, Figure 1b shows four other clusters sampled from a lunar swirl (Fig. 1a). All display a similar trend (Trend A; slopes are approximately –6 ± 1), but each has a distinct saturation color, with the brighter parts of swirls plotting farther down and to the right in Fig. 1b. The downward and rightward displacement of the clusters (Trend B), determined by a best fit line through the centroids, has a slope of –2.0 ± 0.2.

Weathering as a function of latitude: Figure 2 has the same format as Fig. 1b but uses pixels sampled from throughout the lunar maria. To control for varying composition, the data are restricted to regions with high FeO content [10] (to isolate maria from highlands) and similar titanium abundances (based on Lunar Prospector gamma ray data [11]). The points in Fig. 2 are color-coded according to cosine latitude, revealing that the optical characteristics of the surface vary systematically with latitude. Equatorial regions (red dots) tend to have lower albedo and higher 950 nm/750 nm ratios than regions farther from the equator (blue dots). We quantify this trend (Trend C) by separating the data into five bins according to cosine-latitude and fitting a line through the centroids of the five resulting point clusters. The resulting best-fit slope is –1.5 ± 0.2 (black line in Fig. 2).

Discussion: The key result of the above analysis is that the spectral properties of the lunar surface vary with latitude (*cf.* ref 12) and that this variation (Trend C) is quantitatively similar to the trend observed at swirls (Trend B). One interpretation is that both trends are related to a reduction in solar wind flux, which should occur both at high latitudes and in regions with strong magnetic fields (i.e., swirls). Micrometeoroid flux, in contrast, varies with latitude but is unaffected by magnetic fields. This would imply that while micrometeoroid bombardment is responsible for the gradual optical maturation process (Trend A), the rate of micrometeoroid bombardment does not appear to significantly affect the saturation color that is eventually reached. It has also been proposed that the trend observed at swirls (Trend B) could be the result of electrostatic sorting of fine dust or similar mixing of compositionally distinct materials [7–9]. However, if true, this hypothesis would offer no insight into the similar change in color that appears to occur at high latitudes (Trend C).

Conclusions: While this analysis is only preliminary and it remains to be explained why solar wind and micrometeoroid bombardment should have such distinct effects on optical weathering, we regard the relationship between saturation color and latitude, and its resemblance to the spectral trends observed at swirls, as worthy of further study.

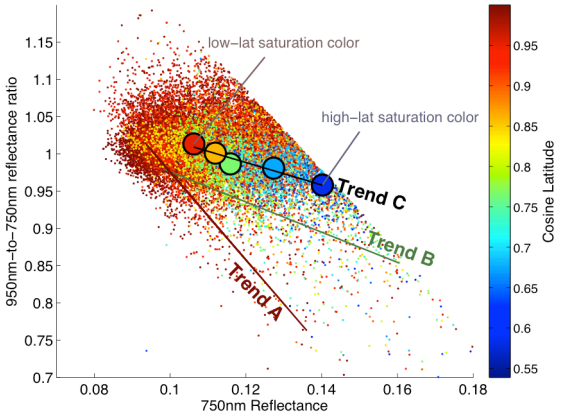

Figure 2: Spectral characteristics of pixels sampled from maria regions of similar composition. Points are colored by cosine latitude (warm colors corresponding to pixels near the equator and cool colors corresponding to pixels away from the equator, up to nearly ±60°). The data are separated into five bins (by cosine latitude) and a large circle is plotted at the centroid of each of the five resulting point clusters. The black line is a best fit through the five centroids and has a slope of –1.5±0.2. The axes are the same as in Fig. 1b. To reduce clutter, only 5% of the data points are plotted. Trend A is difficult to see here since the majority of pixels will correspond to surfaces that have already reached their saturation color.

References: [1] Pieters, C. M. *et al., Meteorit. Planet. Sci.* **35,** 1101–1107 (2000). [2] Hapke, B., *J. Geophys. Res.* **106,** 10,039–10,073 (2001). [3] Vernazza et al., *Nature* **458,** 993–5 (2009). [4] Pieters, C. M. *et al. Nature* **491,** 79–82 (2012). [5] Hood, L. L. & Schubert, G., *Science* **208,** 49–51 (1980). [6] Hood, L. L. & Williams, C. R., *Lunar Planet. Sci. Conf. Proc.* **19,** 99–113 (1989). [7] Garrick-Bethell, I., Head, J. W. & Pieters, C. M., *Icarus* **212,** 480–492 (2011). [8] Blewett, D. T. *et al., J. Geophys. Res.* **116,** (2011). [9] Pieters, C. M., Moriarty, D. P. & Ian Garrick-Bethell., *45th Lunar Planet. Sci. Conf.* (2014). [10] Wilcox, B. B., Lucey, P. G. & Gillis, J. J., *J. Geophys. Res.* **110,** (2005). [11] Prettyman, T. H. *et al., J. Geophys. Res.* **111,** (2006). [12] Yokota, Y. *et al., Icarus* **215,** 639–660 (2011).